Investigation of a Large High-Speed Diesel Engine Transient Behavior Including Compressor Surging and Emergency Shutdown

G. Theotokatos
e-mail: makis@central.ntua.gr

N. P. Kyrtatos

Laboratory of Marine Engineering,
Department of Naval Architecture
and Marine Engineering,
National Technical University of Athens,
P.O. Box 64033,
Zografos 15710, Athens, Greece

The operation of a large high-speed engine under transient loading conditions was investigated, using a detailed simulation code in conjunction with a model capable of predicting compressor surging. Engine loadings were applied, which were considered dangerous for initiating compressor surging and cases where compressor surging could occur were identified. A means of avoiding compressor surging by opening a bypass valve connected between the compressor outlet and turbine inlet was examined. Finally, the case of engine abrupt stopping by rapidly closing the engine emergency shutdown valve, located downstream of the compressor, was also investigated. [DOI: 10.1115/1.1559903]

Introduction

Engine simulation codes are widely used during the design, development and optimization of the reciprocating internal combustion engine, [1–3]. Especially during the recent years, the increasing complexity of engine configurations, [4,5], (using EGR, waste gates or Variable Geometry Turbines) in conjunction with the extensive usage of electronic systems for controlling the various engine parameters, [6], introduced for improving engine performance and reducing exhaust emissions, necessitates the utilization of detailed engine simulation codes in the design process. Using such codes for predicting the steady state as well as the dynamic behavior of the engine and its components, the prototypes manufactured can be designed close to the optimum solution. Detailed engine simulation codes can be used, apart from matching the engine with its turbocharger and testing various engine controllers and engine design options, for investigating the engine and turbocharger transient behavior, [3,7,8], as well as complex phenomena, such as compressor surging, and thus obtaining data which otherwise could only be measured using complicated and costly techniques.

For determining the compressor behavior under surging conditions, a lumped parameter model was introduced in [9]. This model was applied for studying of the dynamics of the surge and rotating stall in an axial flow compression system and was verified experimentally. It was shown in [10], that this model is also applicable to centrifugal compressors. In [11], the compressor shaft speed dynamics were incorporated in the above model, greatly improving the agreement with the surge behavior measured in a turbocharger centrifugal compressor fitted on a single compression system.

In [12], the model presented in [9] was used in conjunction with an engine simulation code for the performance prediction of a sequentially turbocharged marine Diesel engine, including cases where compressor surging occurred. For investigating the turbocharged reciprocating engine behavior under compressor surging conditions, a one-dimensional unsteady flow model was also presented in [13]. This model was capable of predicting the compressor and engine behavior, but the full geometry of the compressor and its piping system is required and it can be only used in conjunction with one-dimensional codes.

The model presented in [11] was extended by the authors, [14,15], so that the variations of the compressor inlet pressure and temperature during compressor surging cycles were taken into account, and was extensively validated against the experimental results published in [11]. This model was incorporated into a detailed zero-dimensional code, [16,17], as a new compressor model, so that the code can be used for examining special cases of engine running under conditions that may result in compressor surging.

The present paper describes the investigation of the transient behavior of an eight-cylinder, 34.5 L, large high-speed Diesel engine, using the derived engine simulation code. After validating the steady-state simulation results against experimental data, initial transient simulation runs were performed in order to compare the derived results using the existent and the new compressor models. Furthermore, the dynamic behavior of the engine and its turbocharger was investigated, with engine loadings that were considered dangerous for compressor surging. In addition, a way for avoiding compressor surging by opening a bypass valve connected between the compressor outlet and the turbine inlet was examined. Finally, the engine and turbocharger behavior during the engine emergency shutdown procedure was also investigated.

Turbocharged Engine Modeling

For the prediction of the steady-state and transient performance of a turbocharged engine, a detailed zero-dimensional code has been developed and used for a number of years, [16,17]. The code is flexible allowing the simulation of a variety of engine configurations including four-stroke, two-stroke, Diesel, gasoline, natural gas, turbocompound engines, etc.

The code is of ''control volume'' (filling and emptying) type, and it can also estimate the one-dimensional flow effects inside engine manifolds based on a pseudo-one-dimensional pipe model. A number of basic engineering elements such as flow receivers (cylinders, plenums), flow controllers (valves, compressors, turbines, heat exchangers, pipes), mechanical elements (crankshaft, shafts, gearboxes, clutches, shaft loads), and controller elements (PID speed governor, PID controllers) are available. A turbocharged engine can be modeled as several flow receiver elements

Contributed by the Internal Combustion Engine Division of THE AMERICAN SOCIETY OF MECHANICAL ENGINEERS for publication in the ASME JOURNAL OF ENGINEERING FOR GAS TURBINES AND POWER. Manuscript received by the ICE Division July 2001; final revision received by the ASME Headquarters Mar. 2002. Associate Editor: D. Assanis.

(control volumes) interconnected by flow controller elements. The engine environment is regarded as a fixed fluid element (constant pressure, temperature and composition). Mechanical connections are allowed between cylinders and crankshaft, which in addition can be connected to a shaft load via a gearbox and/or clutch. Although a number of different submodels are available for the simulation of the various components of an engine, only the ones used for the modeling of the engine examined in this paper will be described here.

The flow receivers are treated as open thermodynamic systems where work, heat, and mass transfer take place through their boundaries. The working fluid in each flow receiver is regarded as homogenous mixture of pure air and combustion products, subjected to the perfect gas law. Spatial uniformity of the fluid properties is assumed at any instant. Thus, the instantaneous state of the flow receiver gas is described by its temperature, equivalence ratio and pressure. The first law of thermodynamics, the conservation of mass and the ideal gas law are applied to each flow receiver. The resulting set of coupled differential equations is numerically solved step by step for all volumes in turn.

The rate of change of a flow receiver gas equivalence ratio with respect to time depends on the rate of fuel addition by injection and on the fuel content in the form of combustion products of the gas entering or exiting the flow receiver.

Combustion is modeled as a heat release process. Cumulative fuel burning rate diagrams (S-curve functions, [18]) are used for the simulation of the combustion process.

The heat transfer process between the working gas and its surroundings is considered to consist of two parts: heat transfer from gas to wall and heat transfer from wall to coolant, for both the flow receiver and the flow controller elements. For the first part, in the case of cylinders, the heat transfer coefficient is calculated using the Woschni correlation, [19], whereas Nu-Re-Pr correlations, [20], are used for calculating the heat transfer coefficient in the other flow receivers and flow controllers. For the wall to coolant heat transfer, the surface wall temperature of the various elements are calculated using coefficients that determine how close the wall temperature is to the ''adiabatic'' temperature of the wall or to the coolant temperature.

In the case of cylinders, the rate of change of a cylinder volume is calculated using the geometry of the piston, crank throw, and connecting rod.

The flow through the inlet and exhaust valves (flow controllers), connected to a flow receiver, is considered to be quasi-steady, [18,21], at each time step and calculated as a function of instantaneous valve effective area and pressure ratio.

The compressor is modeled using a digital representation of its steady-state map. The steady-state compressor map is assumed to apply at all engine operating conditions. The compressor map, which represents the compressor speed and efficiency as functions of corrected flow with respect to pressure ratio, is accessed using the instantaneous values of pressure ratio and turbocharger speed obtained from calculations within the engine simulation program. The compressor corrected flow and efficiency are calculated using interpolation, thus enabling the calculation of the instantaneous compressor mass flow rate. Then, the compressor impeller absorbed torque is calculated by the following equation:

$$\tau_c = \frac{30\gamma R \dot{m}_c T_{o1}}{\pi N(\gamma-1)\eta_c}(pr_c^{(\gamma-1)/\gamma}-1). \tag{1}$$

The turbine is modeled using a digital representation of its swallowing capacity and efficiency maps, which usually provide the turbine swallowing capacity (or mass flow rate parameter) and efficiency, as functions of the turbine pressure ratio and the turbocharger speed. The turbine mass flow parameter and efficiency are calculated using the turbine expansion ratio and the turbocharger shaft speed, interpolating between the given points of the turbine maps. Then, the instantaneous turbine torque is calculated by

$$\tau_t = \frac{\dot{m}_t c_p T_{o3} \eta_t (1-(p_{o4}/p_{o3})^{(\gamma-1)/\gamma}) - \dot{Q}_t}{\pi N/30}. \tag{2}$$

Turbocharger speed is obtained by integrating the angular momentum conservation equation, governing the turbocharger shaft dynamics:

$$\frac{dN_{TC}}{dt} = \frac{30}{\pi I}(\tau_t - \tau_c). \tag{3}$$

The temperature of air exiting the charge air cooler is calculated using the cooler effectiveness. The air cooler pressure drop is calculated as function of the air cooler mass flow rate.

The gas temperature, mass and equivalence ratio of every flow receiver at each time step are calculated by numerically integrating, through a predictor-corrector scheme, the differential equations giving the time derivatives of gas temperature, mass, and equivalence ratio, respectively. The gas pressure is calculated using the perfect gas law.

For the calculation of the engine crankshaft speed, the engine cylinders are considered to be mechanically connected to the crankshaft, which is in turn connected to the engine load. The cylinders produce torque, whereas the engine load absorbs torque. The engine speed is defined by the angular momentum conservation in the engine crankshaft:

$$\frac{dN_E}{dt} = \frac{30(\Sigma_{i=1}^{ncyl}\tau_i - \tau_L)}{\pi I_{tot}}. \tag{4}$$

For the calculation of the brake torque developed by the engine cylinders, friction losses, dependent on the mean piston speed and the maximum cylinder pressure, [22], are taken into account.

For the transient engine simulation, an engine speed governor element is used for the control of the fuel rack position, which, in turn, determines the fuel injected into the engine cylinders in order to stabilize the engine speed around a desired point. The output of the engine speed governor is calculated using the PI control law:

$$y = y_{init} + k_P(N_{ord}-N) + k_I\int_{t_0}^{t}(N_{ord}-N)dt. \tag{5}$$

Compressor Dynamic Response Modeling

In previous studies of the authors, [14,15], a model capable of predicting the compressor dynamic behavior including cases of turbocharger compressor surging was presented. This model was extensively validated using published experimental data for a simple centrifugal compression system.

This model was incorporated into the engine simulation code as an additional compressor model. According to this model, the compressor mass flow rate is calculated using the following equation:

$$\frac{d\dot{m}_c}{dt} = \frac{p_2 - p_p}{L_c/A} \tag{6}$$

where $p_2 = p_1 \cdot pr$.

The above equation was derived considering the compressor as a single pipe and applying the momentum conservation. The cross-sectional area of this pipe is considered to be equal to the compressor impeller eye area and the equivalent length is calculated by

$$\frac{L_c}{A} = \int_{\text{compressor \& its ducting system}} \frac{d\ell}{A(\ell)}. \tag{7}$$

Using the above equations, the inertia of the air contained inside the compressor and its inlet and outlet ducts is taken into account.

In addition, in order to take into account the departure of the compressor characteristics from their steady-state form when the

compressor operates under dynamic conditions, the following first order differential equation is used for the calculation of the compressor pressure ratio:

$$\frac{dpr}{dt}=\frac{1}{\tau}(pr_{ss}-pr). \tag{8}$$

The time lag, used in the above equation, has the effect of flattening the steady-state compressor characteristics, [11,23], and is considered to be in the order of the compressor throughflow time, [11]:

$$\tau=\frac{L_{mer}}{|c|} \tag{9}$$

where L_{mer} is the meridional length of the compressor impeller and diffuser and c is the meridional average flow velocity.

The additional compressor geometric data, required as input for the new model are, the equivalent length (L_c) for the compressor inlet, impeller, diffuser, volute and outlet ducting system, the impeller eye area (A), the compressor impeller and diffuser meridional length (L_{mer}). In addition, the compressor characteristics in the form of pressure ratio versus flow for various values of rotational speed are required. For the calculation of the compressor torque, the nondimensional torque coefficient as a function of flow coefficient, instead of the efficiency contours, was preferred to be used as input. Plotting the compressor nondimensional torque coefficient versus flow coefficient, the result will be almost a straight line. Thus, only the coefficients of the equation of this line must be given as input. For each point of the compressor map, the compressor nondimensional torque coefficient can be calculated by

$$\Gamma_c=\frac{\tau_c}{\rho A r_2 U^2} \tag{10}$$

where the compressor torque is given by Eq. (1), whereas the compressor flow coefficient can be calculated by

$$\phi_c=\frac{\dot{m}_c}{\rho A U}. \tag{11}$$

Thus, the following equation can be used for the estimation of the compressor nondimensional torque, which is derived by curve fitting using the points of Γ_c and ϕ_c, calculated from the compressor map:

$$\Gamma_c=c_1\,\phi_c+c_2. \tag{12}$$

According to the new model, the steady-state compressor map is accessed with the instantaneous values of corrected mass flow rate and corrected speed and the steady-state pressure ratio is calculated using interpolation. The compressor pressure ratio and mass flow rate are calculated at the end of each step by integrating the differential Eqs. (8) and (6), using a predictor corrector scheme. Then, the compressor flow coefficient, the compressor nondimensional torque coefficient and the compressor torque are calculated in turn (Eqs. (11), (12), and (10)). In addition, the compressor efficiency is calculated using Eq. (1). The total temperature at the compressor outlet is calculated by the following equation, which is derived from the energy equation in the compressor, [18]:

$$T_{o2}=T_{o1}+\frac{\tau_c\,\omega}{\dot{m}_c c_p}. \tag{13}$$

The total enthalpy of the air entering the flow receiver connected downstream of the compressor can then be calculated using the temperature T_{o2}.

The instantaneous turbocharger shaft speed is calculated by integrating the angular momentum conservation equation (Eq. (3)) for the turbocharger shaft.

In case where the calculation of the compressor surging cycle is required, the compressor characteristics as well as the nondimensional torque coefficient for the region to the left of the surge line and for negative flows is needed as input.

In that case, for calculating the complete compressor characteristics and the nondimensional torque coefficient versus flow coefficient for the negative compressor flow region, a meanline analysis method was used in [15], which, however, requires a great amount of compressor geometric input data. Alternatively, a method for the estimation of compressor characteristics and nondimensional torque coefficient, when the compressor map for the normal flow region is available, was presented in [14,15]. According to that, the characteristics of a centrifugal compressor can be estimated using the following second-order polynomial equation for the negative flow region:

$$pr=pr_0+\frac{pr_{srg}-pr_0}{\dot{m}_{srg}^2}\dot{m}_c^2 \tag{14}$$

whereas, the following third-order polynomial equation, which was proposed in [24], is used for calculating the compressor characteristics for the region between zero flow and surge line:

$$pr=pr_0+\frac{pr_{srg}-pr_0}{2}\left[1+1.5\left(\frac{2\dot{m}_c}{\dot{m}_{srg}}-1\right)-0.5\left(\frac{2\dot{m}_c}{\dot{m}_{srg}}-1\right)^3\right] \tag{15}$$

where the compressor pressure ratio at zero flow is calculated by the following equation, [14]:

$$pr_0=\left[1+\frac{\gamma-1}{2\gamma RT_{o1}}\omega^2(r_2^2-r_1^2)\right]^{\frac{\gamma}{\gamma-1}}. \tag{16}$$

For the positive compressor flow region, the nondimensional torque coefficient can be estimated using the equation of the line that fits the points of Γ_c and ϕ_c, calculated from the compressor map (Eq. (12)). For the negative compressor flow region the even extension of this function can be used.

For negative compressor flow, the torque absorbed by the compressor impeller, which is derived using the energy equation in the compressor, is given by

$$\tau_c=\frac{|\dot{m}_c|c_p(T_{o1}-T_{o2})}{\omega}. \tag{17}$$

Thus, the total temperature at the compressor inlet is calculated by

$$T_{o1}=T_{o2}+\frac{\tau_c\,\omega}{|\dot{m}_c|c_p}. \tag{18}$$

The total enthalpy of the air entering the compressor inlet volume is calculated using the temperature T_{o1}.

Engine Description

The Caterpillar 3508 (CAT 3508) engine is a four-stroke, large high-speed Diesel engine, [25]. It can be used as a propulsion

Table 1 Caterpillar 3508 parameters

Number of cylinders	8
Cylinder arrangement	60° V
Displacement	34.5 L
Bore	170 mm
Stroke	190 mm
Connecting rod length	380 mm
Compression ratio	13
Turbocharger	1 ABB RR-151
Operating speed range	1200–1800 rpm
Power output	785 kW@1800 rpm
BMEP	15.2 bar
Engine total polar moment of inertia	25.9 kg m^2

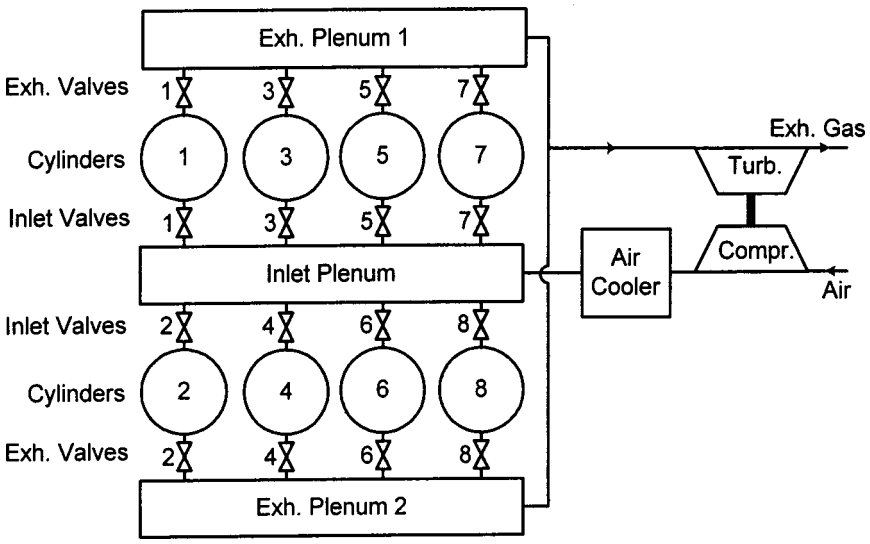

Fig. 1 CAT 3508—engine configuration

plant engine (mainly in tugs, fishing boats, fast ferries, etc.) as well as a generator set engine. A CAT 3508 engine is installed in the testbed of the Laboratory of Marine Engineering (LME) of NTUA, [26], connected to a Zoelner water brake.

The CAT 3508 engine employs the constant pressure turbocharging system. Its intake manifold is located between the two banks of cylinders. The cylinders of each bank discharge their exhaust gas into two different exhaust plenums. The standard production engine has two separate turbochargers, each one connected to the exhaust plenum of one of the two cylinder banks. The CAT 3508 test engine of the LME is equipped with a single ABB RR-151 turbocharger, [27], whose turbine is connected to both exhaust manifolds via a Y-junction. This engine configuration was modeled here.

The basic engine parameters are given in Table 1, whereas the engine configuration is shown in Fig. 1.

Results and Discussion

Initially, steady-state runs for engine operation at 1500 rpm and various loads were performed. The combustion model constants were adjusted so that the measured maximum cylinder pressure as well as the engine torque is adequately predicted. The derived steady-state simulation results are presented in Fig. 2. In the same figure, the respective measured data for the original engine configuration (with two turbochargers) and for the engine configuration with the 1 RR-151 turbocharger, are also given. Good agreement between the measured and the predicted results is observed. However, it must be noted that the turbine of the turbocharger for the simulated configuration was the one that is currently fitted on the engine of the LME testbed, and its nozzle area is smaller than the one of the turbine with which the measurements were performed. Thus, the predicted engine exhaust receiver pressure is

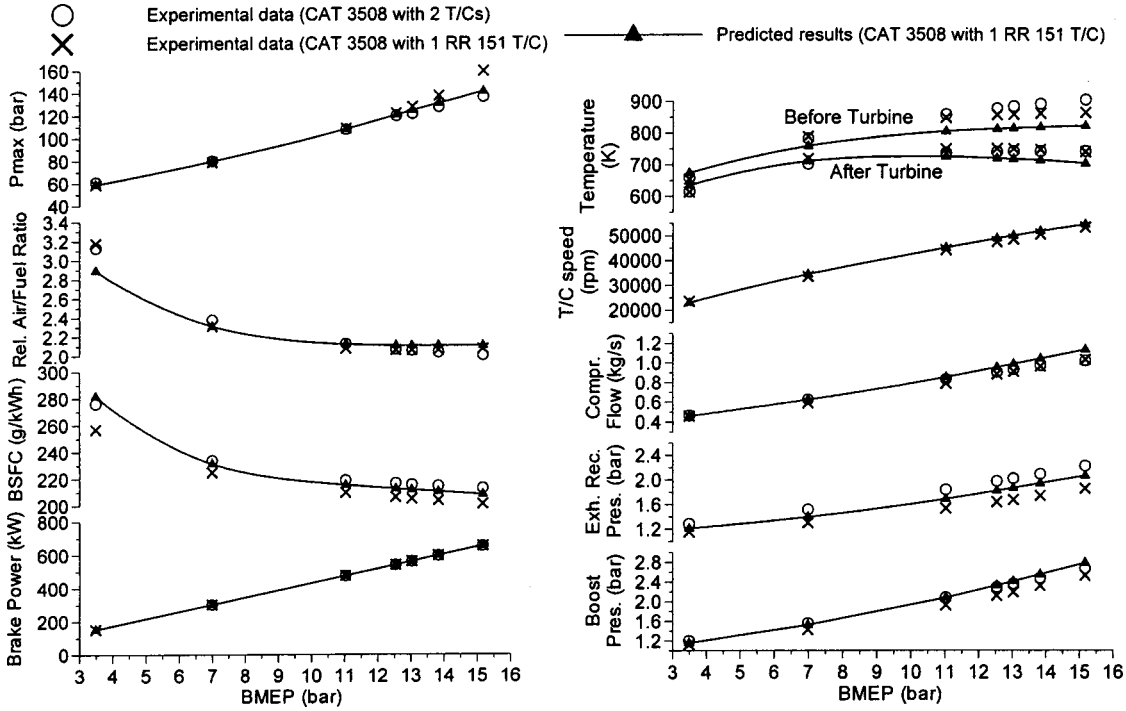

Fig. 2 Steady-state predicted and measured results at 1500 rpm

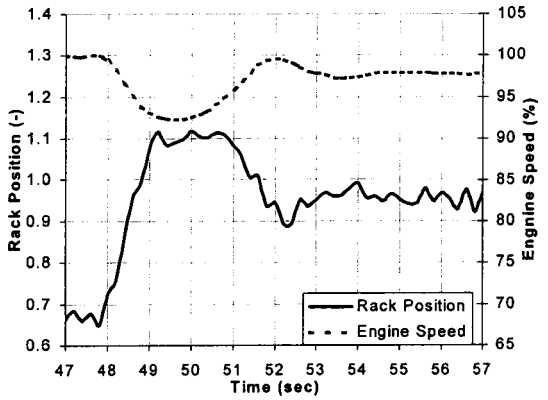

Fig. 3 CAT 3508—measured rack position and engine speed during load increase

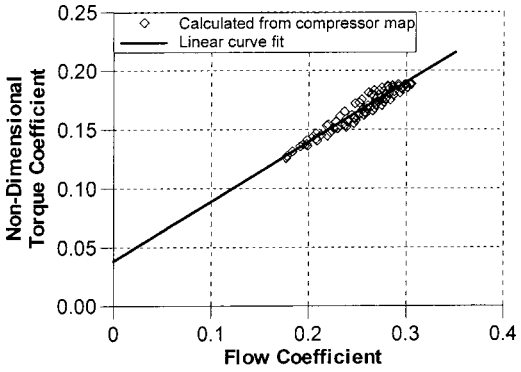

Fig. 4 Compressor nondimensional torque coefficient versus flow coefficient (calculated from compressor map and its linear curve fit)

slightly greater than the measured one, resulting in slightly higher turbocharger speed, compressor mass flow rate and engine boost pressure. Therefore, more air is available in the engine cylinders for burning almost the same fuel amount, having as a result lower exhaust receiver temperature.

After the steady-state simulation, a case of engine transient simulation with load increase from 70% to 100% was examined. For such a case, measured data for the engine fuel rack position and engine speed were available and shown in Fig. 3. Using these data, the engine PI speed governor constants (see Eq. (5)), were calculated so that the predicted results are in good agreement with the measured ones. These values were found to be: $k_P = 0.016$ and $k_I = 0.045$. The transient simulation was performed using the existent compressor model as well as the new compressor model. The compressor nondimensional torque coefficient versus flow coefficient points, which were calculated using the compressor map, are shown in Fig. 4. In this figure, the line, which fitted these data and used as input in the calculations, is also presented. For the predictions of the compressor surge cycles presented below in this text, the even extension of this function was used for estimating the nondimensional torque coefficient for the negative compressor flow region. In addition, the third order polynomial Eq. (15) was used for the estimation of the compressor characteristics between zero flow and the surge line, whereas the compressor characteristics for the negative flow region were taken from [15].

A set of the predicted results for the engine transient from 70% to 100% load, including the engine rack position, the engine speed, the engine torque, the engine brake power, the relative air/fuel ratio, the compressor pressure ratio and the turbocharger speed, as well as the trajectory of the compressor operating points superimposed on the compressor map, is given in Fig. 5. In addition, the variation of the compressor parameters within one engine cycle for the cycles after 0.3 sec (corresponding to 70% load) and after 9.5 sec (corresponding to 100% load) is presented in Fig. 6.

As can be seen from these figures, the engine and turbocharger mean cycle parameters derived using the existent and the new compressor models practically coincide. However, the compressor efficiency values for the engine operating region close to 100%

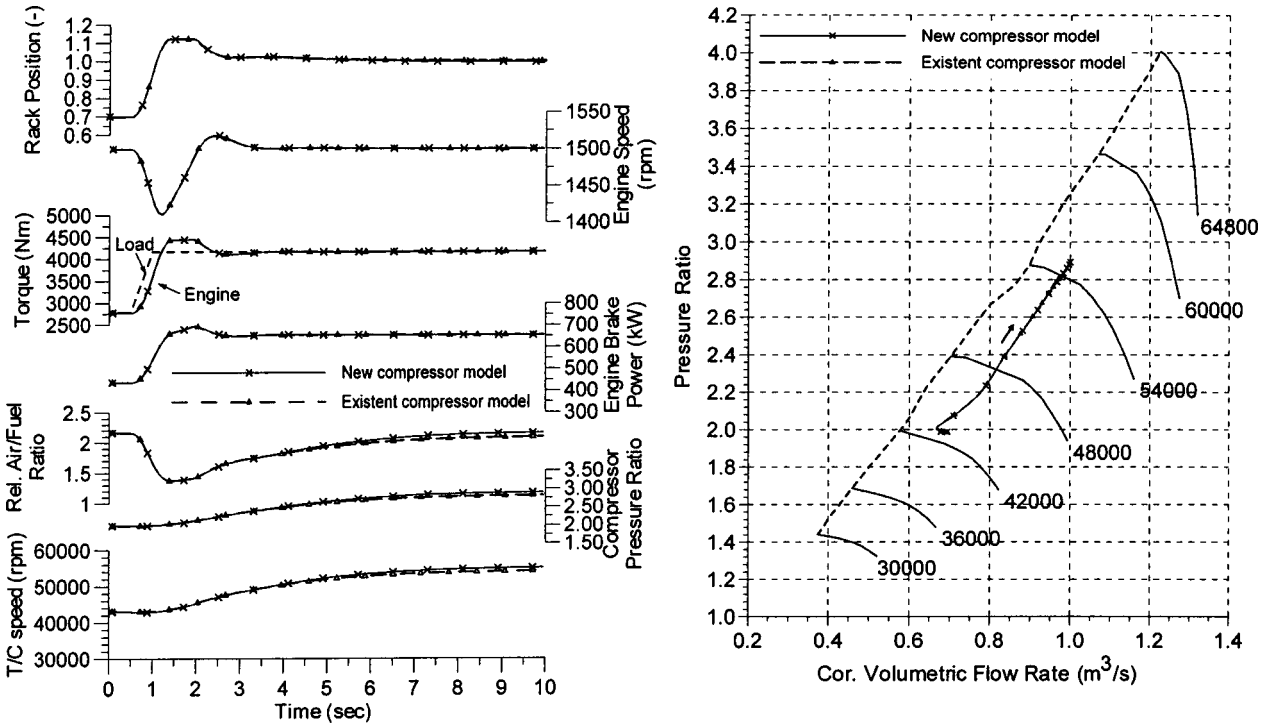

Fig. 5 Simulation results for engine load increase from 70% to 100% at 1500 rpm

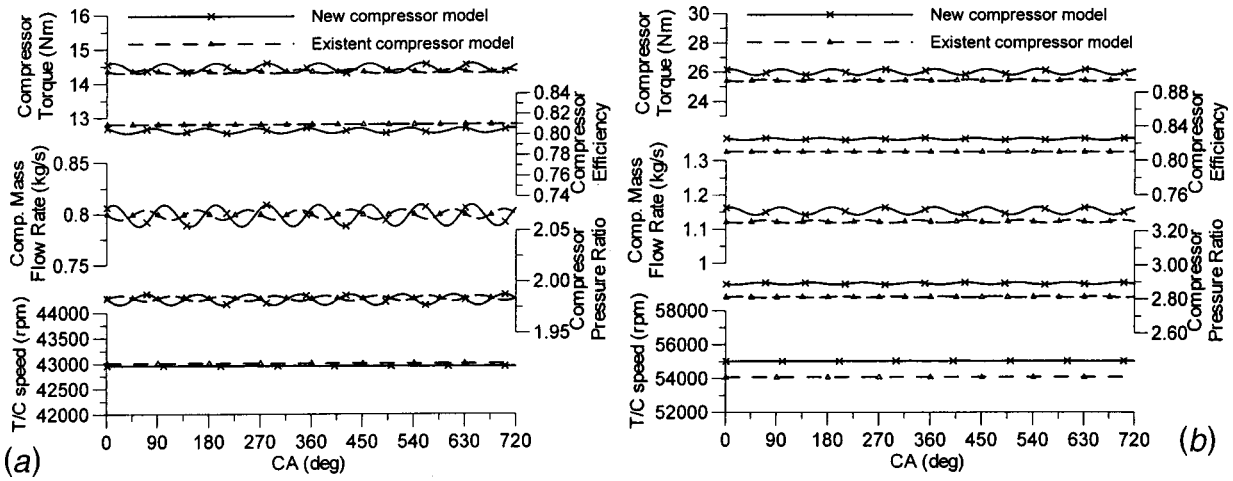

Fig. 6 Compressor parameters versus CA for (*a*) engine cycle after 0.3 sec (70% load) and (*b*) engine cycle after 9.5 sec (100% load)

load, predicted with the new model are slightly greater than the ones predicted with the existent model, resulting in slightly higher turbocharger speed, compressor pressure ratio and air/fuel ratio. In addition, the instantaneous values of the compressor parameters calculated using the new model are slightly shifted, compared to the respective ones calculated using the existent model. The former is owing to the fact that the compressor torque was calculated using the linear fit instead of the points derived directly from the compressor map (Fig. 4). The latter is attributed to the way of calculating the compressor mass flow rate and pressure ratio using Eqs. (6) and (8), instead of calculating the mass flow and pressure ratio directly from the steady-state compressor map. However, since the new compressor model gives mean cycle results comparable to the ones derived using the existent compressor model, and additionally, the inertia of the air inside the compression system passages and the departure of the compressor characteristics from their steady-state form are taken into account, it is expected that more realistic predictions can be derived by using the new model.

Next, a transient run was performed, in which engine load changes, ''dangerous'' for compressor surging, were imposed. The engine was operating at 1500 rpm with 85% load and the engine load was reduced to 10% at 0.5 sec and then increased again to 100% at 2 sec. The predicted engine rack position, engine speed, engine torque and power, relative air/fuel ratio, compressor pressure ratio and turbocharger speed, as well as the trajectory of the compressor operating points on the compressor map are shown in Fig. 7.

During the load reduction[1] from 85% to 10%, the engine speed increased about 10% (1650 rpm at 1 sec) and as a result, the compressor mass flow also increased.[2] Thus, the compressor operating point moved towards the choking region on the compressor map. However, due to the engine speed governor response, the engine speed reached the engine setpoint of 1500 rpm at about 2 sec. At that moment, the engine load increased to 100%, causing

[1]An engine load reduction may result in engine overspeed when the engine operates close to the upper limit of its speed range. However, no problems are encountered in the running of the turbocharger components.

[2]For a four-stroke engine, the engine volumetric air flow rate, and as a result the compressor volumetric flow rate, mainly depends on the engine displacement volume and the engine speed.

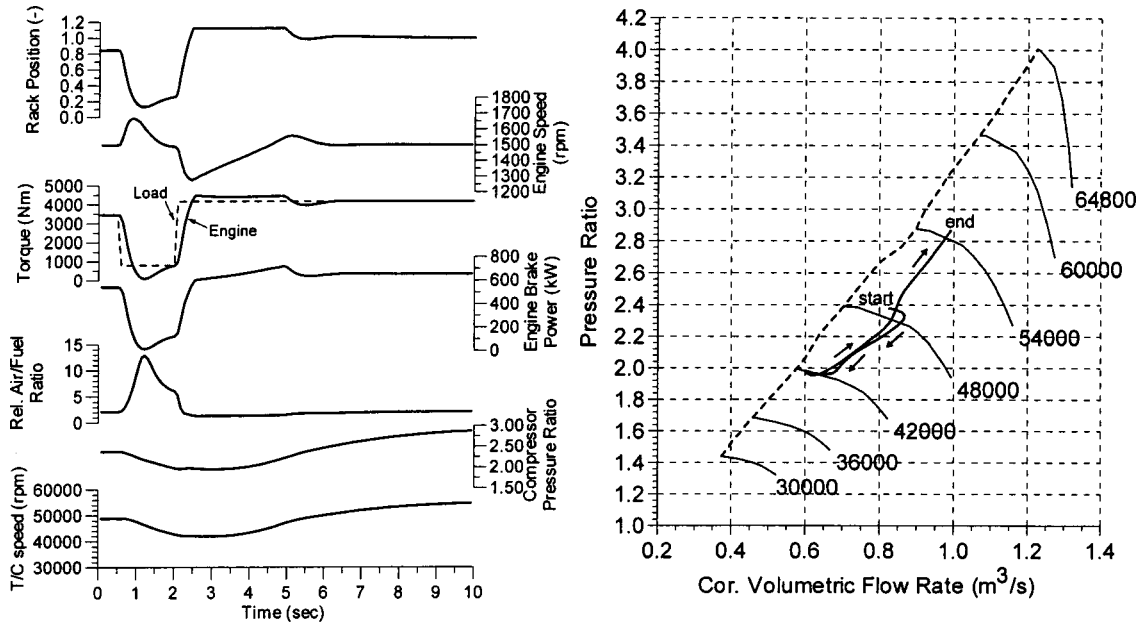

Fig. 7 Simulation results for engine transient operation at 1500 rpm—load changes 85%–10%–100%

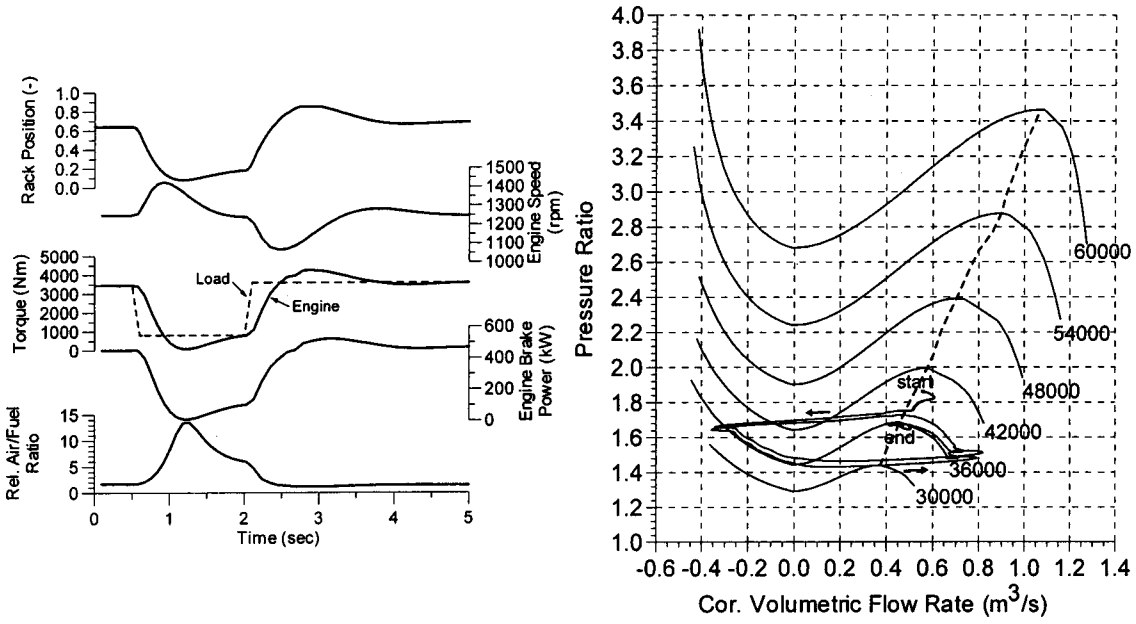

Fig. 8 Simulation results for engine transient operation at 1250 rpm—load changes 85%–10%–90%

an engine speed drop of about 15% (1270 rpm at 2.4 sec). This resulted in the reduction of the compressor mass flow rate, and thus the compressor operating point on the compressor map moved towards the surge line. Subsequently, the engine speed increased due to the action of the engine speed governor, so the compressor mass flow rate increased and as a result the compressor operating point moved away from the compressor surge line.

In the examined case, i.e. with engine running at 1500 rpm, the surge margin was adequate for avoiding compressor surging. However, considering the case where the engine operates at 1250 rpm, the compressor operating point is located closer to the surge line and the surge margin is less than the one for the case of engine running at 1500 rpm. The predicted engine parameters and the trajectory of the compressor operating points, for the case of engine running at 1250 rpm with load changes 85%–10%–90% are given in Fig. 8. The predicted compressor parameters for the same case are shown in Fig. 9 As can be seen from these figures, compressor surging occurred during the engine load increase at about 2.3 sec. At that time, the engine speed had dropped to 1050 rpm, which caused the reduction of the compressor mass flow rate, and thus the compressor operating point moved inside the compressor unstable area. Subsequently, with the increase of the engine speed due to the response of engine governor, the compressor operating point moved again into the compressor stable operating region. As can be seen from Fig. 9, the compressor surge cycle lasted about 0.2 sec and consists of the period of positive to negative flow reversal (where the compressor flow was almost instantaneously reduced from 0.5 kg/s to −0.4 kg/s), the period of negative flow, the period of the negative to positive flow reversal (where the compressor flow almost instantaneously increased from 0 kg/s to 0.95 kg/s), and the recovery period. During the compressor negative flow period, the pressure downstream of the compressor was reduced from 1.75 bar to 1.45 bar within 0.08 sec, and subsequently, after the negative to positive flow reversal, the pressure downstream of the compressor increased again, reaching 1.7 bar at 2.5 sec, before the next compressor surge cycle. As shown in Fig. 9, during compressor surging the torque absorbed by the compressor impeller rapidly varied (especially during the flow reversals), thus introducing severe torsional loadings to the turbocharger shaft. Due to the changes of compressor

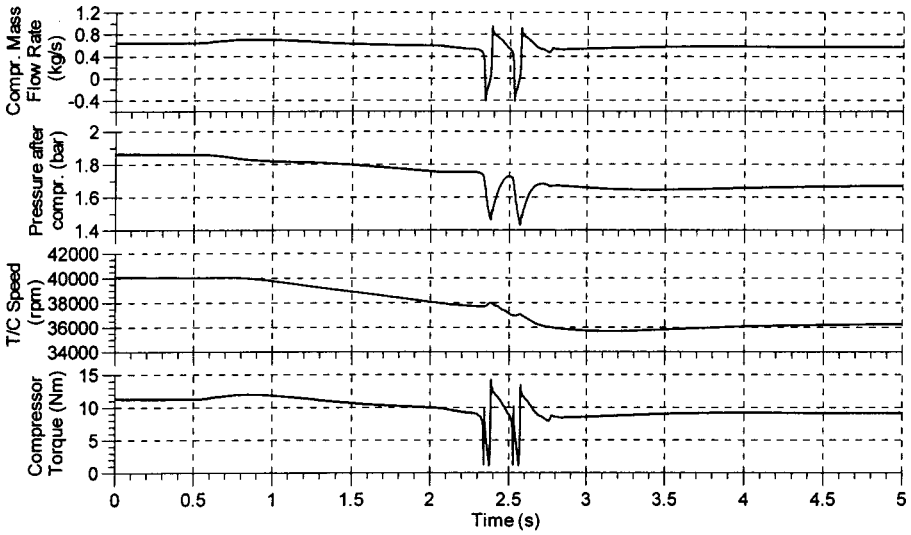

Fig. 9 Predicted compressor parameters for engine transient operation at 1250 rpm—load changes 85%–10%–90%

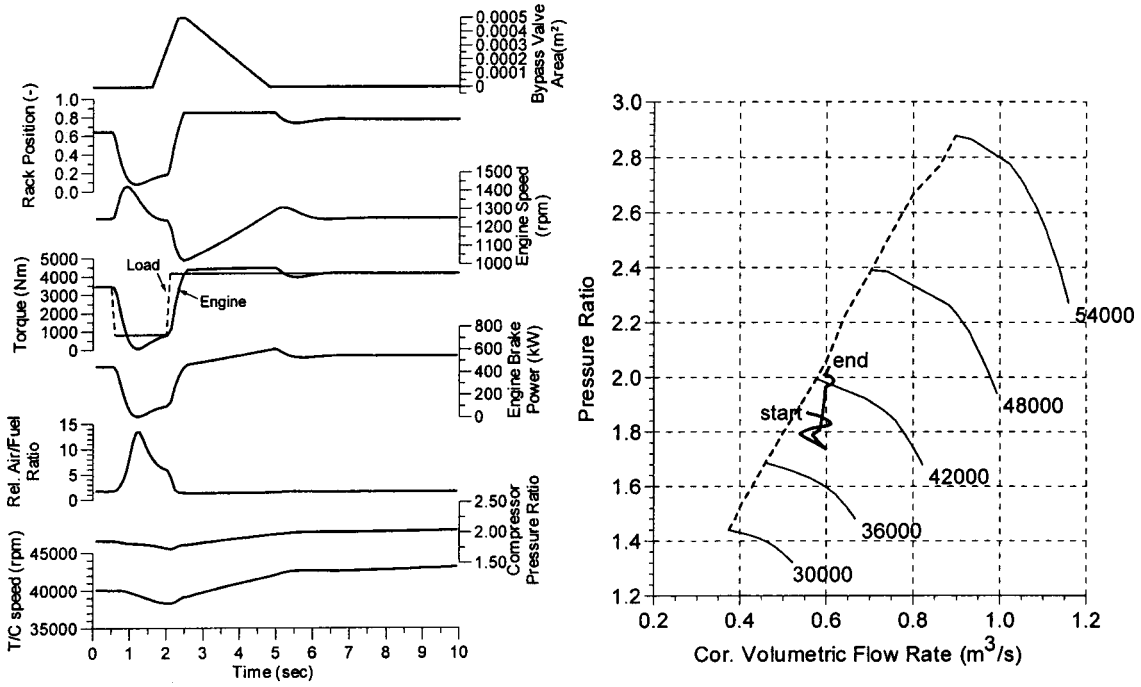

Fig. 10 Simulation results for engine transient operation at 1250 rpm and bypass opening—load changes 85%–10%–100%

torque, the turbocharger speed increased about 200 rpm during the period of negative compressor flow, and was subsequently reduced after the negative to positive flow reversal. It is evident that such flow, pressure, and turbocharger shaft torque oscillations can harmfully influence both the engine and turbocharger operation. In the examined case, the compressor surging lasted less than 0.5 sec, and therefore it cannot critically affect the engine safe running. However, the continuous occurrence of compressor surging can adversely affect the engine running and should be avoided.

A way of avoiding compressor surging, even when the engine operates under dangerous load profiles, is by using a bypass valve, connecting the compressor outlet and the turbine inlet. By opening this valve, some of the compressor air passes into the turbine. In that way, the turbine and also the compressor mass flow rates are greater than the one required by the engine. In addition, since the energy of the bypass air is used by the turbine (and not wasted, as in the case of a simple pressure relief valve), the turbocharger speed also increases. As a result, the compressor operating point moves further away from the surge line.

The predicted engine and compressor parameters and the trajectory of the compressor operating points, for the case of engine running at 1250 rpm with load changes 85%–10%–100% and bypass valve opening, are shown in Fig. 10. The bypass valve was progressively opened starting from about 1.6 sec, just before the forthcoming engine load increase, till the point of minimum engine speed at about 2.3 sec. Thus, the compressor mass flow was

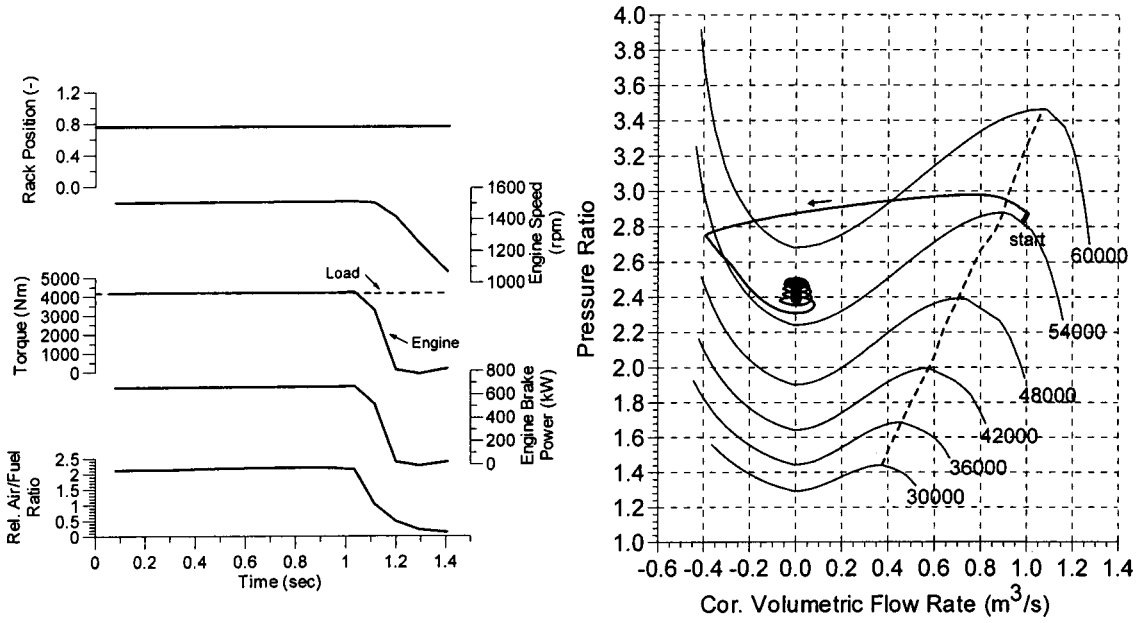

Fig. 11 Simulation results for engine transient operation during emergency shutdown

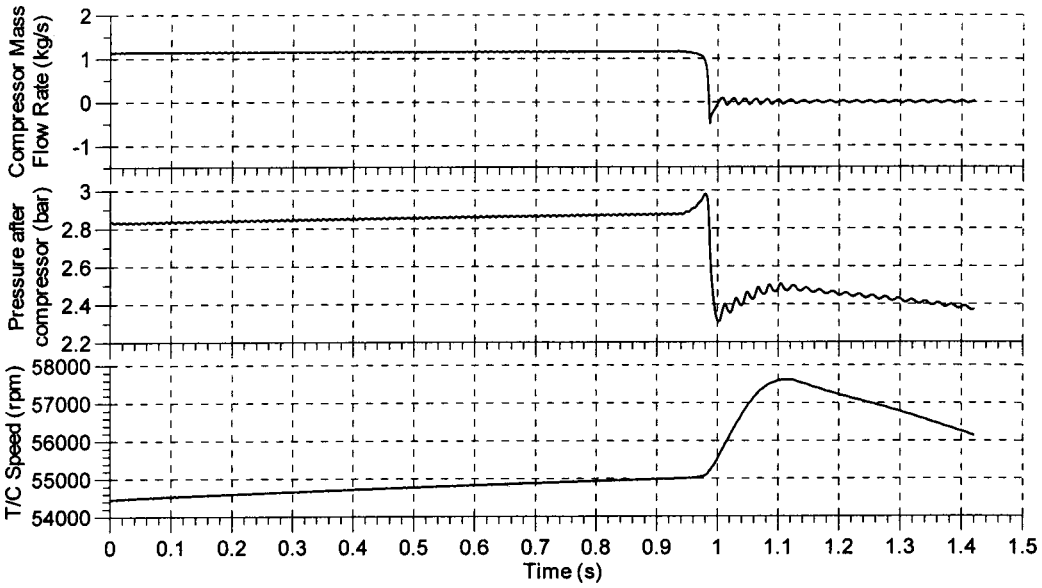

Fig. 12 Predicted compressor parameters for engine transient operation during emergency shutdown

increased and the compressor operating point was moved in an adequate margin away from the surge line at 2 sec. Therefore, the engine speed drop (from 1250 rpm at 2 sec to 1050 rpm at 2.4 sec) did not cause compressor surging. The bypass valve was then progressively closed until its fully closed position at about 4.5 sec, when the engine speed was close to its initial value of 1250 rpm. In addition, as can be seen comparing Figs. 9 and 10, the bypass valve opening also prevented the turbocharger speed reduction for the time period after about 1.8 sec.

Finally, the CAT 3508 engine emergency shutdown was simulated. The engine emergency shutdown valve is located between the compressor outlet and the engine air cooler and it instantaneously closes in any case where an emergency alarm is activated. Thus, the air supply to the engine cylinders is immediately cut and the engine shuts down due to the lack of air to maintain the fuel combustion in the cylinders. The predicted engine parameters and the trajectory of the compressor operating points on the compressor map for such a case are presented in Fig. 11. In addition, the compressor parameters are shown in Fig. 12.

Initially, the engine was operating at 1500 rpm and 100% load. The emergency shutdown procedure was initiated at 0.9 sec. At that instant, the emergency shutdown valve started closing and it fully closed at 1 sec. As Fig. 11 and Fig. 12 show, during the closing of the emergency shutdown valve, the pressure after the compressor was gradually increased, from 2.85 bar at 0.94 sec to almost 3 bar at about 0.98 sec. Therefore, the compressor operating point was driven into the compressor unstable region, and the compressor flow rate became almost instantly negative at about 0.98 sec. However, the surge cycle was not completely followed, since after the negative to positive flow reversal (at about 1 sec), the shutdown valve had been fully closed, so the compressor flow became almost zero. Due to flow reversal, the pressure after compressor was reduced to 2.3 bar at 1 sec, whereas the turbocharger speed increased, from 55,000 rpm at 0.98 sec to 57,600 rpm at about 1.1 sec, because the compressor impeller absorbed torque was reduced due to the reduction of the compressor mass flow. It was only after 1.1 sec that the turbocharger speed was reduced due to the reduction of the exhaust gas energy, which resulted in the reduction of the turbine torque. After the closing of the shutdown valve, and due to the turbocharger rotation, the pressure after compressor followed the changes of the turbocharger shaft speed, i.e., it increased from 2.3 bar at 1 sec to 2.5 bar at 1.1 sec, and then started decreasing since the turbocharger shaft decelerated.

The closing of the emergency shutdown valve resulted in lack of air for combustion (the relative air/fuel ratio dropped below 0.6, which is the limit for combustion). Thus, the engine torque was reduced (almost to 0 within 0.2 sec), and since the load torque was considered to be constant, the engine rapidly decelerated.

Conclusions

The behavior of a four-stroke, large high-speed engine was examined using a detailed engine simulation code in conjunction with a model capable of predicting the compressor dynamic behavior including cases of compressor surging. Initially, the simulation code steady-state results were validated against experimental data. Then, the engine speed governor model was calibrated based on available engine transient measurements. After that, engine transient simulation using the existent as well as the developed compressor models was performed. Subsequently, additional transient runs were performed, in which, ''dangerous,'' for compressor surging, engine load profiles were imposed. Furthermore, a way of avoiding compressor surging by appropriately opening a bypass valve connecting the compressor outlet and the turbine inlet was examined. Finally, the case of the engine emergency shutdown was also investigated.

The main conclusions derived from the present study are as follows:

The engine simulation code combined with the new compressor model can be used for predicting the engine and its turbocharger dynamic behavior providing more realistic compressor transient performance predictions because the inertia of the air inside the compressor passages as well as the departure of the compressor characteristics during transients from their steady-state form are now taken into account. In addition, the engine and turbocharger behavior can be predicted even in cases where the compressor exhibits surging as well as during engine emergency shutdown.

Engine load profiles dangerous for causing compressor surging were identified. The transient simulation results showed that compressor surging can occur under certain loading conditions if there is inadequate compressor surge margin, thus designating the limits for the engine safe operation. In that respect, the results of this study are used from the LME in order to avoid conditions in the CAT 3508 engine testbed that could lead into compressor surging and thus endanger the integrity of the test unit.

During compressor surging, the compressor mass flow rate exhibits large amplitude oscillations, resulting in also severe fluctua-

tion of the pressure downstream of the compressor, which can adversely affect the turbocharger and engine operation. In addition, the almost instant changes of the compressor absorbed torque can introduce severe torsional loading to the turbocharger shaft.

Compressor surging can be avoided by appropriately opening a bypass valve connecting the compressor outlet and the turbine inlet. In such case, the simulation code can provide the required data for designing a controller for the bypass valve.

The simulation of the engine operation with compressor surging as well as the engine emergency shutdown provides results that cannot be easily measured and thus contributes to the better understanding of the dynamic behavior of the engine and its turbocharger in such cases.

Nomenclature

A = area (m^2)
U = compressor impeller tip velocity (m/s)
c = velocity (m/s), constants
c_p = specific heat at constant pressure (J/kg K)
k = constants
L = length (m)
m = mass (kg)
$\dot{m}$ = mass flow rate (kg/s)
p = pressure (N/m^2)
pr = pressure ratio
$\dot{Q}$ = heat transfer rate (kW)
R = gas constant (J/kg K)
r_1 = impeller eye mean geometric radius (m)
r_2 = impeller tip radius (m)
T = temperature (K)
t = time (s)
y = rack position
Γ = Nondimensional torque coefficient
γ = ratio of specific heats
η = efficiency
I = polar moment of inertia ($kg\,m^2$)
N = rotational speed (rpm)
ϕ = flow coefficient
ρ = density (kg/m^3
τ = time constant (s), torque (Nm)
ω = angular speed (rad/s)

Subsripts

o = total conditions
0 = zero flow
1 = compressor inlet
2 = compressor outlet
3 = turbine inlet
4 = turbine outlet
c = compressor
E = engine
I = I-constant
$init$ = initial
$ncyl$ = number of cylinders
mer = meridional
L = load
ord = ordered
P = P-constant
p = plenum
srg = at surge line
ss = steady state
TC = turbocharger
t = turbine
tot = total

References

[1] Watson, N., and Banisoleiman, K., 1987, ''Computers in Diesel Engine Turbocharging System Design,'' IMechE, C05/87.
[2] Sams, T., Regner, G., and Chmela, F., 2000, ''Integration of Simulation Tools to Optimize Engine Concepts,'' Motortech. Z., (9), pp. 601–608.
[3] Bartsch, P., Prenninger, P., and Allmer, I., 1998, ''Transient Performance Optimization of Turbocharged Engines by Means of Gas Exchange Simulations,'' *IMechE International Conference on Turbocharging and Air Management Systems*, C554/016/98, IMechE, London, pp. 237–251.
[4] Klingmann, R., Fick, W., and Bruggemann, H., 1999, ''The new Common Rail Direct Injection Diesel Engines for the updated E-class Part 2: Combustion and Engine Management,'' Motortech. Z., **No. 7/8-1999**, pp. 426–437.
[5] Biaggini, G., Buzio, V., Ellensohn, R., and Knecht, W., 1999, ''The New Iveco Cursor 8 Diesel Engine,'' Motortech. Z. **No. 10-1999**, pp. 640–649.
[6] Hild, O., Fieweger, K., Pischinger, S., Rake, H., and Schlosser, A., 1999, ''The Controlled System of a Direct-Injection Diesel Engine for Passenger Cars with Regard to the Control of Boost Pressure and Exhaust Gas Recirculation,'' Motortech. Z., **No. 3-1999**, pp. 186–192.
[7] Filipi, Z. S., Wang, Y., and Assanis, D. N., 2001, ''Effect of Variable Geometry Turbines on Diesel Engine and Vehicle System Transient Response,'' SAE Paper No. 2001-01-1247.
[8] Kyrtatos, N. P., Politis, G., Lambropoulos, V., Theotokatos, G., Xiros, N., Coustas, J. D., 1998, ''Optimum Performance of Large Marine Engines Under Extreme Loading Conditions,'' *22nd CIMAC International Congress*, May 18–21, Copenhagen, CIMAC, Frankfurt, **6**, pp. 1539–1553.
[9] Greitzer, E. M., 1976, ''Surge and Rotating Stall in Axial Flow Compressors. Part I: Theoretical Compression System Model,'' ASME Journal of Engineering for Power, **98**, pp. 190–198.
[10] Hansen, K. E., Jørgensen, P., and Larsen, P. S., 1981, ''Experimental and Theoretical Study of Surge in a Small Centrifugal Compressor,'' ASME Journal of Fluids Engineering, **103**, pp. 391–395.
[11] Fink, D. A., Cumpsty, N. A., and Greitzer, E. M., 1992, ''Surge Dynamics in a Free-Spool Centrifugal Compressor System,'' ASME J. Turbomach. **114**, pp. 321–332.
[12] Chesse, P., Hetet, J. F., Tauzia, X., Roy, P., and Inozu, B., 1998, ''Performance Simulation of Sequentially Turbocharged Marine Diesel Engines with Applications to Compressor Surge,'' *Proceedings of ASME ICE Spring Technical Conference*, ASME, New York, **30-2**, pp. 31–40.
[13] Skopil, M., and Bulaty, T., 1998, ''Calculation of Compressor Surge With Unsteady Flow Model,'' *IMechE International Conference on Turbocharging and Air Management Systems*, C554/018/98, IMechE, London, pp. 219–225.
[14] Theotokatos, G., and Kyrtatos, N.P., 2001, ''Diesel Engine Transient Operation with Turbocharger Compressor Surging,'' SAE Paper No. 2001-01-1241.
[15] Theotokatos, G., 2001, ''Analysis of Turbocharger Operation Including Compressor Surging During Transient Loading of Marine Diesel Engines,'' Dr. Eng. Thesis, Department of Naval Architecture and Marine Engineering/ National Technical University of Athens, Athens, Greece.
[16] Kyrtatos, N. P., and Koumbarelis, I., 1994, ''Performance Prediction of Next-Generation Slow Speed Diesel Engines during Ship Manoeuvers,'' Trans IMarE, **106**, Part 1, pp. 1–26.
[17] Kyrtatos, N. P., ed., 1999, *MOtor THERmodynamics Ver 1.3–USER MANUAL*, PRD Ltd., Athens.
[18] Watson, N., and Janota, M. S., 1982, *Turbocharging the Internal Combustion Engine*, Macmillan, London.
[19] Woschni, G., 1967, ''Universally Applicable Equation for the Instantaneous Heat Transfer Coefficient in the Internal Combustion Engine,'' SAE Paper No. 670931.
[20] Rohsenow, W. M., Hartnett, J. P., and Ganic, E., 1985, *Handbook of Heat Transfer Fundamentals*, 2nd Ed., McGraw-Hill, New York.
[21] Heywood, J. B., 1988, *Internal Combustion Engines Fundamentals*, McGraw-Hill, New York.
[22] Ciulli, E., 1992, ''A Review of Internal Combustion Engine Losses, Part 1: Specific Studies on the Motion of Pistons, Valves and Bearings,'' Proc. IMechE, **206**, pp. 223–236.
[23] Wachter, J., and Lohle, M., 1984, ''Experimental Investigation of the Dynamic Behavior of Centrifugal Compressors,'' Stability, Stall and Surge in Compressors and Pumps, D. Japikse, ed., ASME, New York, ASME FED-Vol. 19, pp. 23–30.
[24] Moore, F. K., and Greitzer, E. M., 1986, ''A Theory of Post-Stall Transients in Axial Compression Systems—Part I: Development of Equations,'' ASME J. Eng. Gas Turbines Power, **108**, pp. 68–76.
[25] Caterpillar Co., 1981, ''Technical Information Release—The 3508 Engine'', TIR 10-381, 6/81.
[26] Kyrtatos, N. P., Ioannidis, I. P., Pavlidis, V., Ventouris, K., and Raptis, D., 2001, ''The New Laboratory Facility ''MARTHA'' for Marine Propulsion Research and Development'', 23rd *CIMAC World Congress*, May 7–10, Hamburg, CIMAC, Frankfurt, pp. 1566–1575.
[27] Naguib, M., 1986, ''Experience With the Modern RR 151 Turbocharger for High-Speed Diesel Engines,'' *IMechE Conference on Turbocharging and Turbochargers*, C99/86, IMechE, London, pp. 105–112.